Numerical investigation of the potential of tailored inclusions as noise reduction measures

IOP Conf. Series: Journal of Physics: Conf. Series **1264** (2019) 012013 doi:10.1088/1742-6596/1264/1/012013

Numerical investigation of the potential of tailored inclusions as noise reduction measures

F Mittermeier, J Schauer, M Miksch and G Müller

Chair of Structural Mechanics, Department of Civil, Geo and Environmental Engineering, Technical University of Munich, Arcisstraße 21, 80333 Munich

E-mail: franzi.mittermeier@tum.de

Abstract. The reduction of noise and vibrations is an important task in automotive and aircraft industry. Various applications require slender or adjustable reduction measures. Metamaterials formed by a periodic assembly of unit cells consisting of non-homogeneous material decomposition and having topology dependent favorable absorption properties can meet this need. The absorption efficiency of different types of metamaterials has already been proven by various authors. Thereby metamaterials formed by a periodic assembly of tuned mass dampers on plate-like structures or porous layers with rigid inclusions have been investigated. Beyond that, we suggest to design metamaterials consisting of inclusions containing appropriately tuned mass dampers embedded in a material layer and to examine their noise reduction potential. It is investigated, whether besides absorbing energy by exciting the damping device, the orientation of the tuned mass damper is active by purposefully deflecting waves inside the structure. The analysis is carried out applying the Wave Finite Element Method. Using the inverse approach of the Wave Finite Element Method, stop bands, i.e. frequencies for which no free wave propagation is observed, are detected. In a parameter study, the influence of the characteristics of the inclusion on the absorption behavior of the metamaterial is determined.

1. Introduction

Diverse applications in automotive and aircraft industry require slender noise and vibration reduction measures. Current research shows that acoustic metamaterials can meet those requirements. Thereby the term metamaterial describes a structure having either specifically designed geometric characteristics or material composition which lead to physical behavior that cannot be observed among usual systems. Often, the term is used in conjunction with infinite periodic structures consisting of repetitive unit cells. By appropriately shaping the unit cell, so called stop bands, being frequencies where no free wave propagation occurs, can be observed. The occurrence of these stop bands can be explained by two different approaches: First, destructive interference between transmitted and reflected waves can impede wave propagation in certain frequency ranges. Second, stop bands can be caused by local resonances which, for example, are induced by adding tuned mass dampers to the structure of the unit cell [1].

Various studies show that modifications of the unit cell lead to a manipulation of the wave propagation in the periodic structure. [1-2] show that a periodic assembly of tuned mass dampers (TMDs) on a plate can cause stop bands. The frequency range of the stop bands depends on the characteristics of the TMD, i.e. mass, spring stiffness and damping. [3-5] investigate the

absorption behavior of porous structures containing a periodic assembly of circular inclusions filled with homogeneous material. While the thickness of a porous layer without inclusions has to equal at least one quarter of the wavelength of the excitation in order to effectively attenuate it [3], [3-5] observe absorption peaks below the quarter-wavelength frequency for the structures with circular inclusions. [3] moreover shows that a C-shaped rigid inclusion will further improve the low frequency absorption characteristics in comparison to the circular inclusion. [6] also studies the influence of embedding inclusions in porous layers receiving similar results. Here, besides performing numerical simulations, the results were also confirmed experimentally.

Beyond that, this contribution investigates, whether embedding inclusions containing TMDs in a material layer will effectively increase the noise reduction potential of periodic metamaterials. Both, the influence of the inclusion shape as well as of the TMD orientation on the wave propagation in the periodic structure are studied carrying out numerical simulations using the Wave Finite Element Method (WFEM). As our objective is to adapt the shape of the inclusion and the alignment and material properties of the TMD in order to damp specific excitations properly, the inclusion containing a TMD is termed tailored inclusion.

After having introduced the topic, chapter 2 shows the system to be considered and discusses how the wave propagation in periodic structures is determined. Chapter 3 comprises the results of the numerical studies and reveals the influence of the inclusion shape and the orientation of the contained damping devices on the wave propagation characteristics within the periodic structure. Finally, chapter 4 summarizes the key findings and gives an outlook on further research.

2. Investigation of wave propagation in periodic structures using the WFEM

After characterizing the system of observation to be modeled, this section describes the approach we use to investigate the wave propagation in periodic structures. The WFEM depicts a combination of the conventional Finite Element Method (FEM) and the Bloch Theorem (BT) and particularly dates back to [7-11]. Using the WFEM, all calculations can be carried out considering a single unit cell only, instead of modeling the whole periodic structure. The cell itself is characterized by its stiffness and mass matrices which are determined using the FEM. The periodicity is described by applying boundary conditions according to the BT.

2.1. Problem description

The considered system is a periodic metamaterial shown in figure 1. The two-dimensional unit cell consists of a solid cell with an inclusion which contains a TMD. The structure is periodic with respect to the $x-$direction. For all investigations, the center of gravity of the inclusion coincides with the center of gravity of the cell. In the scope of this contribution, the TMD is characterized by mass and spring stiffness only, the damping is set to zero. As our objective is to investigate the influence of the shape of the inclusion and of the direction of the TMD on the wave propagation within the structure, different inclusion shapes and TMD alignments are studied.

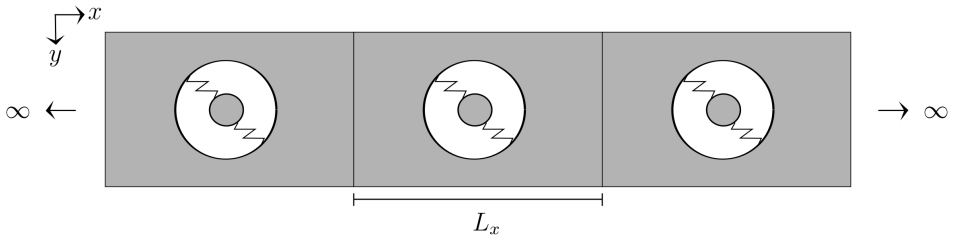

Figure 1. Metamaterial formed of periodic assembly of tailored inclusions embedded in solid material layer.

2.2. Finite Element Method
Each unit cell is characterized by its equation of motion under steady state harmonic loading:

$$(\mathbf{K} - \omega^2\mathbf{M})\mathbf{u} = \mathbf{f}, \tag{1}$$

whereby $\mathbf{K}$ and $\mathbf{M}$ are the stiffness and mass matrices of the unit cell; $\mathbf{u}$ depicts the vector of the degrees of freedom and $\mathbf{f}$ is the force vector; ω is the frequency of observation.

The matrices $\mathbf{K}$ and $\mathbf{M}$ related to the unit cell can be specified using any standard FEM implementation.

2.3. Bloch Theorem
The BT, often also termed Floquet theorem, is used to describe the periodicity of the structure. Being based on [12, 13], it states that the response function of a periodic structure can be expressed via the response function of a single unit cell and an exponential term which describes the change in amplitude and phase as the wave travels from one cell to the next, where the relative change in amplitude and phase between adjacent cells does not depend on the position of these cells within the periodic structure [7]. Consequently the relation between the response functions of two adjacent cells can be expressed as

$$\mathbf{u}(x + L_x) = \mathbf{u}(x)\mu = \mathbf{u}(x)\mathrm{e}^{-i\kappa L_x}, \tag{2}$$

where $\mathbf{u}$ depicts the degrees of freedom of the unit cell. L_x is the length of the unit cell and μ the propagation constant. The wavenumber κ is a complex unity and can be expressed as $\kappa = \kappa_R + i\kappa_I$. Depending on the value of κ, the exponential term can be assigned to three different wave types regarding their propagation characteristics. While $\kappa_I = 0$ results in propagating waves, $\kappa_R = 0$ corresponds to evanescent waves, being near fields that do not undergo any oscillation but decay straightaway. Damped oscillating waves, termed as attenuating waves, occur if both $\kappa_I \neq 0$ and $\kappa_R \neq 0$. The different types of waves are shown in figure 2. While the propagation characteristics of the waves are determined by the values of κ_R and κ_I, the sign of κ_R and κ_I determines the propagation direction.

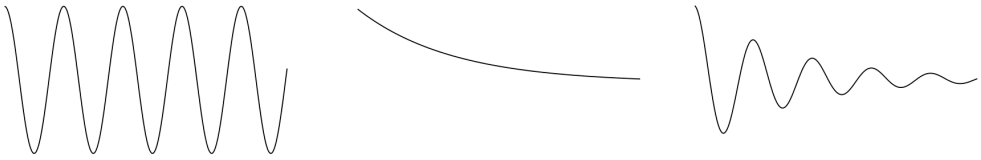

Figure 2. Distinction of waves regarding their propagation characteristics.

We would like to remark that a representation equivalent to equation (2) can be found for the forces acting within the periodic structure.

2.4. WFEM - Inverse approach
Combining the FEM and the BT, the WFEM comprises two common approaches to investigate the dispersion properties of periodic structures: While the direct approach computes the wavenumber for a certain value of frequency, the inverse approach solves for the frequency at a given wavenumber. A further difference between the two approaches is that using the inverse approach only propagating waves are taken into account. Therefore, the inverse approach is an appropriate method to detect stop bands, which correspond to frequency ranges where free wave

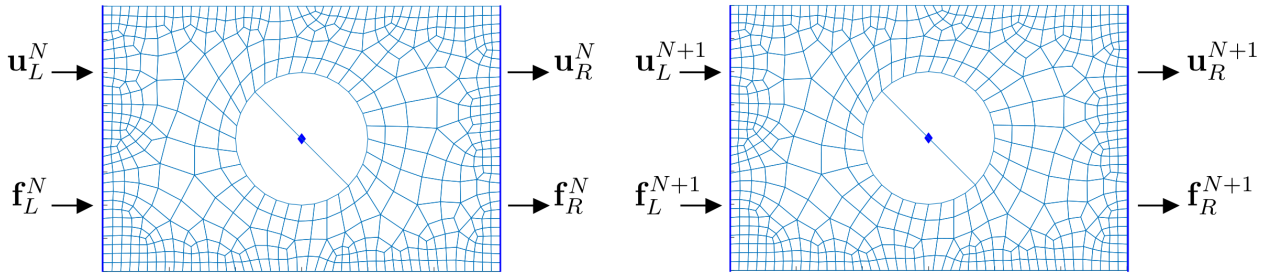

Figure 3. State variables at the boundaries of two adjacent unit cells.

propagation is impeded, and will be used in the context of this contribution. As κ_I consequently vanishes, the propagation constant μ can be simplified:

$$\mu = \mathrm{e}^{-i\kappa_R L_x}. \tag{3}$$

The degrees of freedom and forces related to the single unit cells are distinguished into quantities at the left and right boundary of the cell and internal quantities. The interaction of the boundary degrees of freedom and forces corresponding to two adjacent unit cells is shown in figure 3. Imposing the BT (equation (2)) on these quantities yields:

$$\mathbf{u}_R = \mu \mathbf{u}_L \tag{4}$$

$$\mathbf{f}_R = -\mu \mathbf{f}_L \tag{5}$$

As a result, equation (1) can be reduced to

$$\mathbf{R}^H(\mathbf{K} - \omega^2\mathbf{M})\mathbf{R}\mathbf{u}^{red} = \mathbf{R}^H\mathbf{f}. \tag{6}$$

Here, the reduction matrix $\mathbf{R}$ and its complex conjugate transpose $\mathbf{R}^H$ are introduced. Using equations (4) and (5), $\mathbf{R}$ can be defined as:

$$\mathbf{R} = \begin{bmatrix} \mathbf{I} & \mathbf{Z} \\ \mathbf{Z} & \mathbf{I} \\ \mu\mathbf{I} & \mathbf{Z} \end{bmatrix}, \tag{7}$$

where $\mathbf{Z}$ is the null matrix and $\mathbf{I}$ is the identity matrix. Furthermore, $\mathbf{u}^{red}$ can be found using equation (6):

$$\mathbf{u} = \begin{bmatrix} \mathbf{u}_L \\ \mathbf{u}_I \\ \mathbf{u}_R \end{bmatrix} = \begin{bmatrix} \mathbf{I} & \mathbf{Z} \\ \mathbf{Z} & \mathbf{I} \\ \mu\mathbf{I} & \mathbf{Z} \end{bmatrix} \begin{bmatrix} \mathbf{u}_L \\ \mathbf{u}_I \end{bmatrix} = \mathbf{R}\mathbf{u}^{red}. \tag{8}$$

As no external forces act at the location of the internal degrees of freedom, $\mathbf{f}_I$ is zero and the expression $\mathbf{R}^H\mathbf{f}$ vanishes. Introducing $\mathbf{K}^{red} = \mathbf{R}^H\mathbf{K}\mathbf{R}$ and $\mathbf{M}^{red} = \mathbf{R}^H\mathbf{M}\mathbf{R}$, the equation of motion of the periodic structure can be expressed as

$$(\mathbf{K}^{red} - \omega^2\mathbf{M}^{red})\mathbf{u}^{red} = 0. \tag{9}$$

Given a value for μ, equation (9) depicts a generalized eigenvalue problem of ω^2.

3. Numerical investigations

This section summarizes the results of our numerical investigations. Besides studying the influence of the shape of the inclusion, we have examined whether the alignment of the TMD modifies the dispersion characteristics of the periodic metamaterial (figure 1). For all calculations, the solid part of the unit cell is made of aluminum; the material properties are specified in table 1.

Table 1. Material properties of solid part of unit cell.

Name	Symbol	Value
Young's modulus	E	70 GPa
Density	ρ	2699 kg/m^3
Poisson's ratio	ν	0.34

3.1. Influence of inclusion shape

First, the influence of the inclusion shape on the wave propagation within the periodic structure is investigated. Therefore, the dispersion characteristics corresponding to the three inclusion shapes shown in figure 4 are determined. Besides a circular and a rectangular inclusion, a rhombic inclusion is examined. In this first step no TMD is installed into the inclusion.

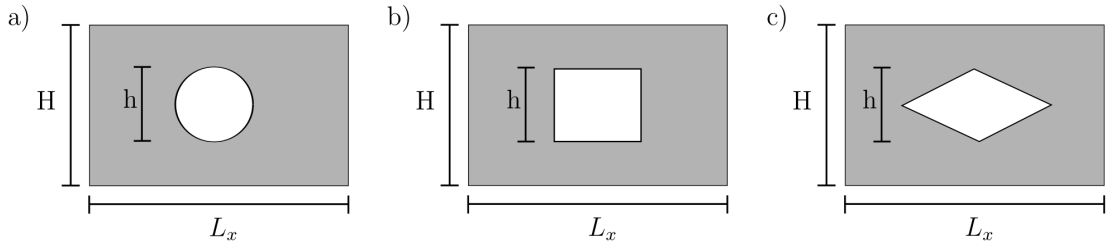

Figure 4. Different inclusion shapes to be considered: a) circle, b) rectangle, c) rhombus.

The inclusions are characterized by their height h and area A. In order to only investigate the influence of the shape and not of the mass loss due to the inclusion, the same height and area is assigned to all inclusion types. Furthermore, all inclusions are located in the center of the unit cell. The length L_x and height H of the unit cell are equal for all configurations. Table 2 summarizes all dimensions of the unit cell.

Table 2. Dimensions of unit cell.

Name	Symbol	Value
Period	L_x	0.06 m
Cell height	H	0.04 m
Inclusion height	h	0.02 m
Inclusion area	A	3.14e-4 m^2

Figure 5 shows the dispersion characteristics of a homogeneous unit cell without inclusion in a frequency range from 0 to 45 kHz. The lines, here termed dispersion curves or bands, mark

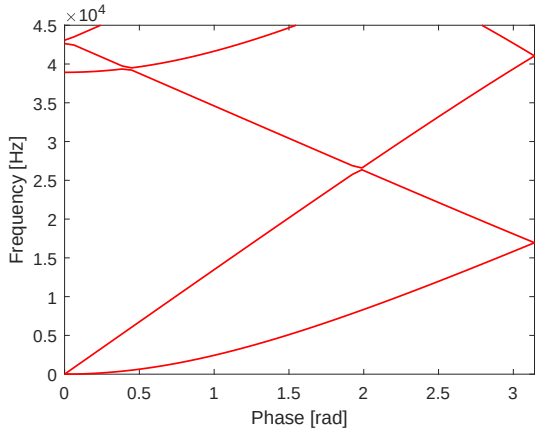

Figure 5. Dispersion curves for homogeneous unit cell.

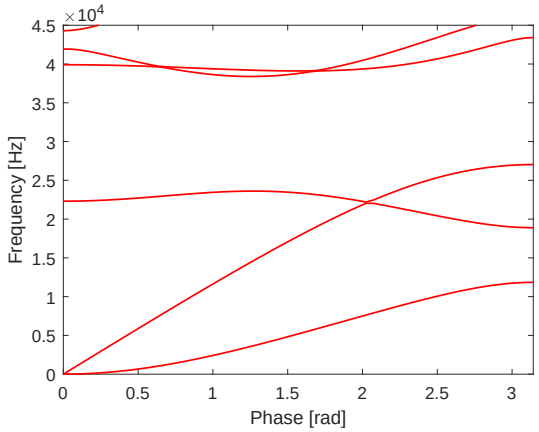

Figure 6. Dispersion curves for unit cell with circular inclusion.

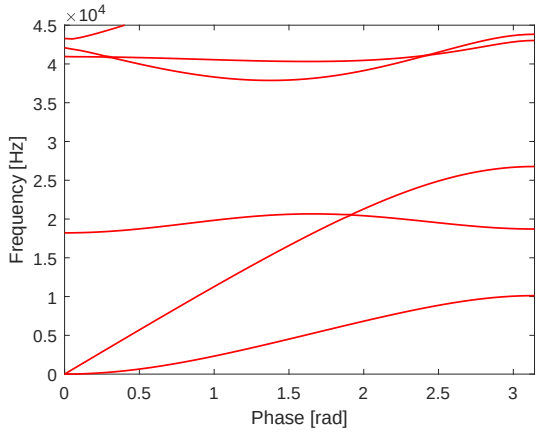

Figure 7. Dispersion curves for unit cell with rectangular inclusion.

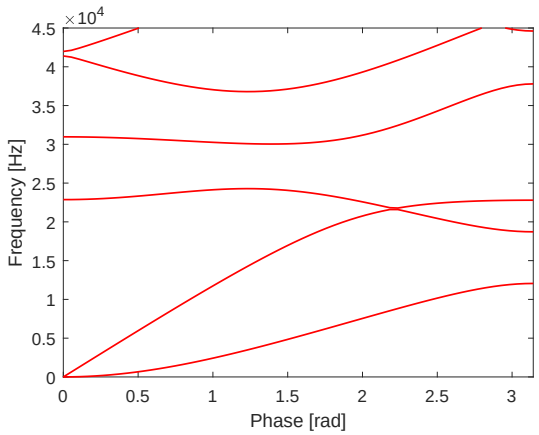

Figure 8. Dispersion curves for unit cell with rhombic inclusion.

the frequencies for which freely propagating waves exist. The phase equals $\kappa_R L_x$ and describes the relative phase shift between two neighboring cells. Taking reference to their shape, the dispersion curves can be assigned to different wave types. Besides dispersive bending waves, non dispersive quasi-longitudinal waves occur for the problem of observation. As the structure is limited with respect to y, it is evident that no pure shear or longitudinal waves are observed. According to figure 5, two bands start from the origin. Since the slope of the lower band is not constant, the corresponding wave is a dispersive bending wave. The curve of the upper band is approximately linear. The respective wave speed can be calculated from the slope of the band as 5090 m/s. Comparing the result to the wave speed of a quasi longitudinal wave, given in equation (10) [14], the upper band is identified as quasi longitudinal wave.

$$c_L = \sqrt{E/\rho} \tag{10}$$

As both, material composition and geometry do not change with respect to L_x, obviously no stop bands occur.

Figures 6 to 8 show the dispersion characteristics of unit cells containing a circular, rectangular and rhombic inclusion. In comparison to the homogeneous unit cell, a stop band is

observed, whereas the width depends on the inclusion shape. Figure 9 compares the stop bands corresponding to the three inclusion types. While the rhombic inclusion leads to the thinnest stop band, the total stop band width for the circular and rectangular inclusion is similar.

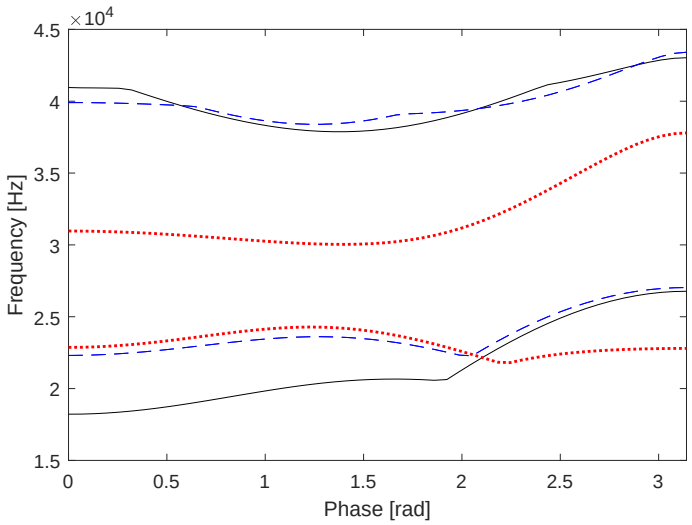

Figure 9. Comparison of stop band width for different inclusion types: (- - -) circle, (—) rectangle and (···) rhombus.

The dispersion characteristics of the different inclusion shapes can be explained taking reference to the different mass distribution with respect to x. Figure 10 shows the mass distribution for all kinds of inclusions over the length of the cell. The mass density on the y-axis

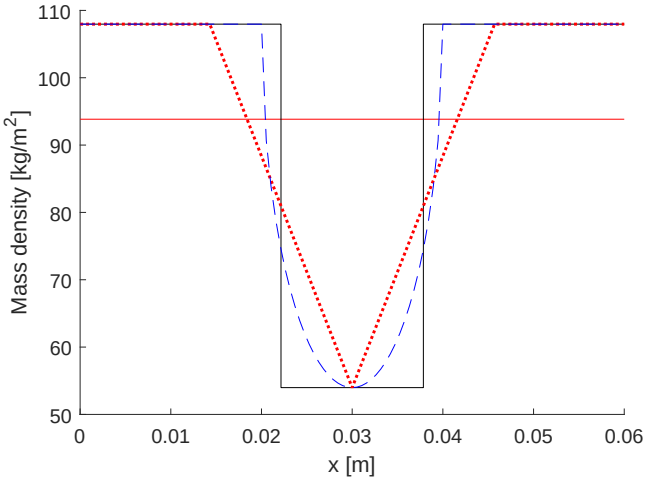

Figure 10. Distribution of mass with respect to x: (- - -) circle, (—) rectangle and (···) rhombus; (—) marks the average mass distribution.

equals the density assigned to the cell multiplied with the material filled height (total height minus local inclusion height). The average mass distribution can be determined as $\rho\frac{(HL_x)-A}{L_x}$ and is also shown. Using the functions of the mass distribution with respect to x, the variance of the mass distribution corresponding to the different inclusion types is gained as

$$Var(X) = \int_0^{L_x} (X - E(X))^2 dx. \tag{11}$$

Here, X equals the mass distribution and $E(X)$ the average mass distribution. Table 3 summarizes the variances corresponding to the different inclusion shapes. The result leads to the conclusion that the stop band width tends to increase with increasing variance. Though this might be true for the geometry configurations investigated within this contribution, further studies are needed to confirm this statement.

Table 3. Variance of mass distribution corresponding to different inclusion shapes.

Inclusion shape	Variance
Circle	26.87
Rectangle	33.22
Rhombus	18.53

3.2. Influence of TMD orientation

This subsection studies the influence of the alignment of the TMD on the wave propagation in the periodic metamaterial. For this analysis, a circular inclusion is chosen. Figure 11 shows the TMD-alignments to be considered. As the damping is set to zero, the TMDs are modeled by

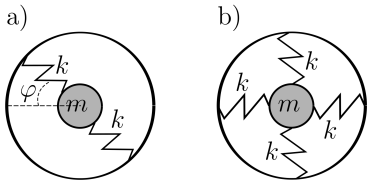

Figure 11. Spring alignments to be considered: a) single-spring inclined by angle φ, b) double-spring.

spring(s) and a concentrated mass. Besides a TMD with a spring which is inclined by an angle φ, a configuration with two orthogonal springs (termed as double-spring) is examined. The mass is located in the center of the spring(s). It is assumed that the mass moves only along the direction of the spring(s). The material configuration of mass and spring(s) will not be changed during the investigations. While the mass equals $A\rho = 0.85$ kg, which is the mass that has been removed from the unit cell due to embedding the inclusion, the spring stiffness is chosen as 1.20 GN/m. According to equation (12) the first eigenfrequency of all TMD configurations equals 8457 Hz.

$$f = \frac{1}{2\pi}\sqrt{\frac{2k}{m}} \tag{12}$$

Figure 12 compares the dispersion characteristics of a cell with circular inclusion without TMD and with TMD which is inclined by $\varphi = \frac{\pi}{4}$. A straight dotted line marks the eigenfrequency of the TMD. It can be seen that both, the bending and quasi longitudinal wave are deflected due to the TMD. Furthermore, figure 12 shows that the TMD particularly affects the frequency

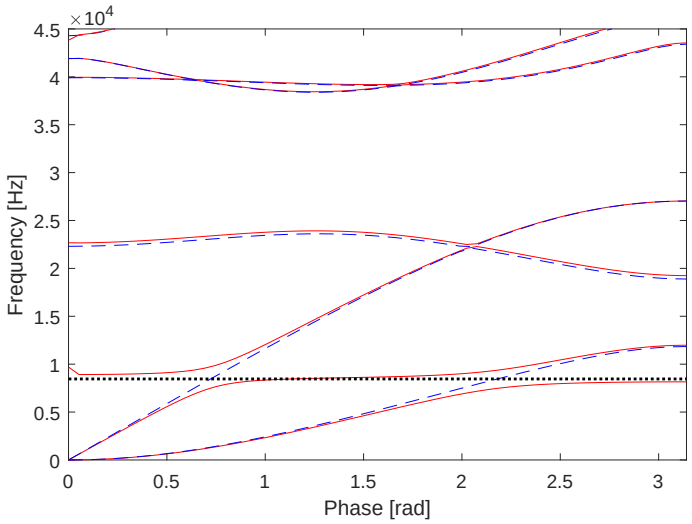

Figure 12. Dispersion curves for unit cell with circular inclusion (- - -) without TMD and (—) with single-spring TMD inclined by $\frac{\pi}{4}$; (···) marks the eigenfrequency of the TMD.

range below the stop band. Consequently, in the following we will concentrate on that frequency range.

In comparison to figure 12, figures 13 and 14 display the dispersion characteristics of a TMD inclined by $\varphi = 0$ and $\varphi = \frac{\pi}{2}$. While a horizontal TMD only deflects the quasi longitudinal wave, a vertical TMD only modifies the band corresponding to the bending wave. Figure 15 shows that those limit cases merge into one another when varying φ between 0 and $\frac{\pi}{2}$. Furthermore, figure 16 verifies that, as the system is symmetric, an inclination φ of $\frac{\pi}{4}$ and $-\frac{\pi}{4}$ will lead to the same result. This statement holds for all pairs $\pm\varphi$.

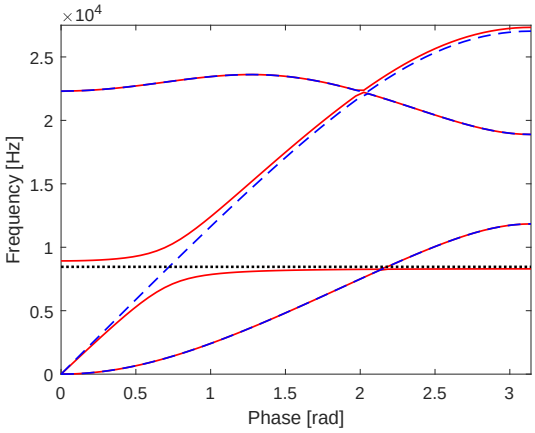

Figure 13. Dispersion curves for unit cell with circular inclusion (- - -) without TMD and (—) with single-spring TMD inclined by 0; (···) marks the eigenfrequency of the TMD.

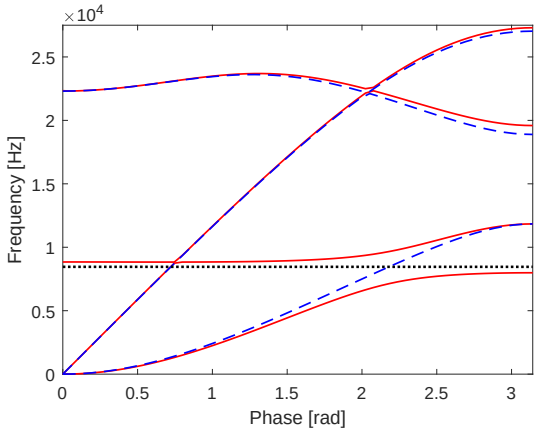

Figure 14. Dispersion curves for unit cell with circular inclusion (- - -) without TMD and (—) with single-spring TMD inclined by $\frac{\pi}{2}$; (···) marks the eigenfrequency of the TMD.

The observed behavior can be explained taking reference to the direction of particle motion corresponding to the different wave types. The part of wave energy transferred into the TMD

will increase with increasing compliance of the direction of wave motion and spring force. While the forces within a horizontal spring coincide with the direction of particle motion of quasi longitudinal waves, the forces within a vertical spring match the direction of particle motion corresponding to bending waves.

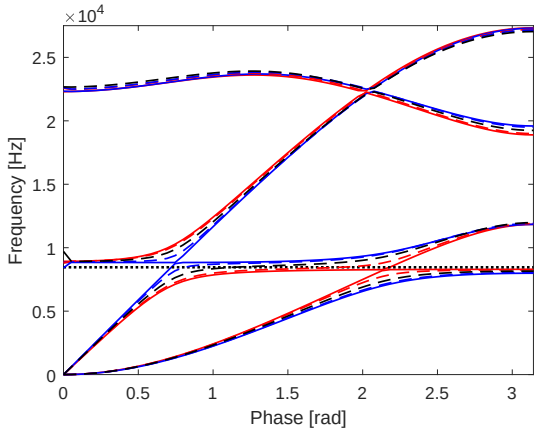

Figure 15. Dispersion curves for unit cell with circular inclusion and single-spring TMD inclined by (—) 0, (- - -) $\frac{\pi}{8}$, (- - -) $\frac{\pi}{4}$, (- - -) $\frac{3\pi}{8}$ and (—) $\frac{\pi}{2}$; (···) marks the eigenfrequency of the TMD.

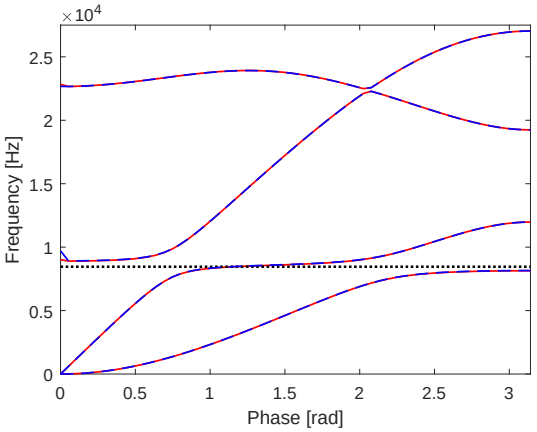

Figure 16. Dispersion curves for unit cell with circular inclusion and single-spring TMD inclined by (- - -) $\frac{\pi}{4}$ and (- - -) $-\frac{\pi}{4}$; (···) marks the eigenfrequency of the TMD.

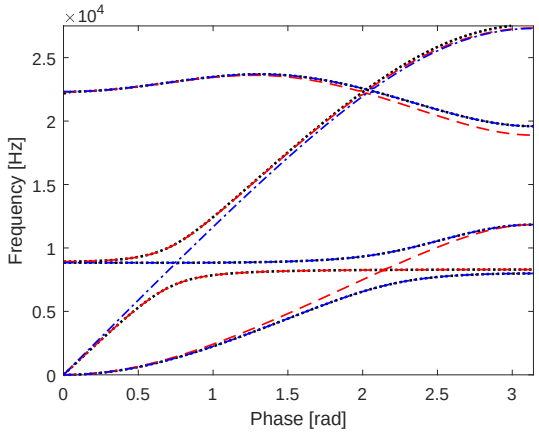

Figure 17. Dispersion curves for unit cell with circular inclusion with single-spring TMD inclined by (- - -) 0, (- - -) $\frac{\pi}{2}$ and (···) with double-spring TMD.

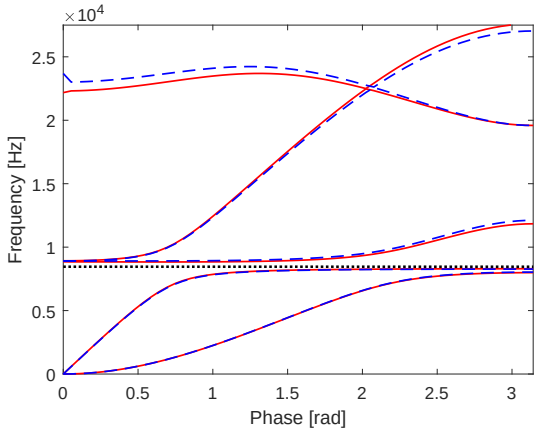

Figure 18. Dispersion curves for unit cell with circular inclusion and (—) double-spring TMD and (- - -) double-spring TMD inclined by $-\frac{\pi}{4}$; (···) marks the eigenfrequency of the TMD.

As introduced in figure 11, in addition to a single-spring TMD, a TMD consisting of a double-spring system is considered. Figure 17 compares the dispersion curves corresponding to the double-spring configuration shown in figure 11 to those of TMDs with single springs inclined by $\varphi = 0$ and $\varphi = \frac{\pi}{2}$ respectively. While for single-spring TMDs no total stop band at the eigenfrequency of the TMD was observed, for the double-spring system a stop band at the

eigenfrequency occurs. Spring forces in direction of the particle motion corresponding to both, quasi longitudinal and bending wave explain the observed behavior.

As long as the two springs have the same spring stiffness and are orthogonal with respect to each other, the portion of spring stiffness in horizontal and vertical direction is not modified by an inclination of the double-spring. Figure 18 confirms that inclining the double-spring system will not change the dispersion curves in the area of the eigenfrequency of the TMD.

4. Conclusion and outlook

Investigating the influence of the inclusion shape and the TMD alignment on the dispersion characteristics of the observed metamaterial with tailored inclusions leads to the following conclusions:

- For inclusions of the same area, the shape of the inclusion influences the dispersion characteristics.
- For the geometry and material configurations applied within this contribution, the stop band width tends to increase with an increasing variance of the mass distribution.
- Varying the inclination of a single-spring TMD, waves can be influenced purposefully.
- To gain a total stop band at the eigenfrequency of the TMD, a double-spring system is needed.

Though these conclusions hold within this contribution, they need to be verified by further studies including the evaluation of different dimensions of unit cell and inclusion, different material properties and more complex systems.

The next steps will include the visualization of the deformed unit cell corresponding to the respective location on the dispersion curve: This extension will lead to a better understanding of the complex process of wave propagation within periodic structures. Furthermore, later studies will deal with the investigation of porous unit cells with tailored inclusions. Thereby we expect that a porous unit cell, in comparison to a solid cell, enhances the absorption behavior of the considered metamaterial.

References

[1] Claeys C, Vergote K, Sas P and Desmet W 2012 On the potential of tuned resonators to obtain low-frequency vibrational stop bands in periodic panels *Journal of Sound and Vibration* **332** 1418-36
[2] Claeys C, Rocha de Melo Filho N G, Van Belle L, Deckers E and Desmet W 2016 Design and validation of metamaterials for multiple structural stop bands in waveguides *Extreme Mechanics Letters* **312** 7-22
[3] Deckers E, Claeys C, Atak O, Groby J-P, Dazel O and Desemet W 2016 A wave based method to predict the absorption, reflection and transmission coefficient of two-dimensional rigid frame porous structures with periodic inclusions *Journal of Computational Physics* **312** 115-38
[4] Groby J-P, Wirgin A and Ogam E 2008 Acoustic response of a periodic distribution of macroscopic inclusions within a rigid frame porous plate *Waves in Random and Complex Media* **18** 409-33
[5] Groby J-P, Dazel O, Duclos A, Boeckx L and Kelders L 2011 Enhancing the absorption coefficient of a backed rigid frame porous layer by embedding circular periodic inclusions *J. Acoust. Soc. Am.* **130** 3771-80
[6] Nennig B, Renou Y, Groby J-P and Aurégan Y 2012 A mode matching approach for modeling two dimensional porous grating with infinitely rigid or soft inclusions *J. Acoust. Soc. Am.* **131** 3841-52
[7] Brillouin L 1946 *Wave propagation in periodic structures* (New York: McGraw-Hill Book Company)
[8] Mead D J 1973 A general theory of harmonic wave propagation in linear periodic systems with multiple coupling *Journal of Sound and Vibration* **27** 235-60
[9] Mace B R, Duhamel D, Brennan M J and Hinke L 2005 Finite element prediction of wave motion in structural waveguides *J. Acoust. Soc. Am.* **117** 2835-43
[10] Orris M R and Petyt R 1974 A finite element study of harmonic wave propagation in periodic structures *Journal of Sound and Vibration* **33** 223-36
[11] Langley R S 1993 A note on the force boundary conditions for two-dimensional periodic structures with corner freedoms *Journal of Sound and Vibration* **167** 377-81

[12] Floquet G 1833 Sur les équations différentielles linéaires à coefficients périodiques *Ann. scientifiques de l'É.N.S* 2^e *série* **12** 47-88
[13] Bloch F 1929 Über die Quantenmechanik der Elektronen in Kristallgittern *F. Z. Physik* **52** 555-600
[14] Möser M and Kropp W 2010 *Körperschall* (Berlin Heidelberg: Springer-Verlag)